Application of Hilbert-Huang Transforms in Analyzing Pavement Vehicle Interaction

Habtamu Zelelew[1] and Tom Papagiannakis[2]

ABSTRACT

Pavement roughness is one of the dominant attributes of pavement condition affecting public perception of serviceability. It is also the main reason for heavy vehicle dynamic excitation and the generation of dynamic axle loads. In this paper, the Hilbert-Huang Transform (HHT) was utilized to analyze the interaction between roughness profile and dynamic axle loads. Roughness profile data were obtained using an inertial profilometer on five pavement sites with IRI roughness ranging from 0.88 to 3.17 m/km. The dynamic axle load data was collected at three operating speeds, namely 38, 60.5 and 79 km/h using a 5-axle semi-trailer equipped with an air suspension on the drive axles and a rubber suspension on the trailer axles. The size of the dataset allows a maximum of 10 frequency decomposition levels for each test site with a maximum detectable frequency of 4 cy/m. The extent of variation in roughness and dynamic axle loads for each of the frequency sub-bands was summarized through Hilbert energy defined as the sum of squares of the observations. The Hilbert normalized energy was also used to characterize the overall effects of roughness profile, suspension type, and vehicle speed on vehicle dynamics. Regardless of vehicle speeds and pavement roughness levels, the rubber suspension impacts much higher energy per unit length traveled than the air suspension. In conclusion, analyzing pavement roughness profile and dynamic axle loads using the HHT method provides an innovative look at the interaction between pavement roughness profile and heavy vehicle dynamic loads.

Keywords: Pavement roughness, Dynamic load, Hilbert-Huang transforms, and Hilbert energy.

[1] (Corresponding Author) Visiting Assistant Professor, University of Minnesota Duluth, Department of Civil Engineering, 1303 Ordean Court, Duluth, MN 55812, Phone: (218)-726-8427, Fax: (218)-726-8581, E-mail: hzelelew@d.umn.edu.

[2] R.F. McDermott Professor and Chair, Department of Civil and Environmental Engineering University of Texas at San Antonio, One UTSA Circle, San Antonio, TX 78249, Phone: (210)-458-7517, Fax: (210)-458-6475 , E-mail: at.papagiannakis@utsa.edu.

INTRODUCTION

Pavement roughness is considered as one of the dominant attributes of pavement condition affecting public perception of serviceability. In addition, it is the main contributor to heavy vehicle dynamics particularly the dynamic axle loads imparted on pavement surfaces (Papagiannakis et al., 1988). Understanding the effects of pavement roughness on heavy vehicle dynamics is important in designing both vehicles and pavements.

Traditionally, pavement vehicle interaction in the frequency domain has been studied through Fourier transforms (Papagiannakis and Gujarathi, 1995). A limitation of the Fourier approach is that it yields spectra based on the complete duration of the signals being analyzed. The Fourier approach assumes the input data as stationary signal. As a result, the transformed signal has no spatial or time reference. In the context of analyzing pavement vehicle interactions, this means that the effect of localized pavement profile disturbances could be totally masked and their effect on vehicle dynamics lost over a long pavement section. Furthermore, Fourier transforms do not allow a direct comparison between the extent of variation of roughness and truck dynamic axle loads over the range of frequencies studied.

Recently, wavelet transforms have gained popularity in analyzing the effects of pavement surface characteristics on passenger car ride and vehicle dynamics (Zelelew and Papagiannakis, 2009). Several studies have demonstrated that spectral analyses based on wavelets yield better time-frequency resolutions for non-stationary signals than Fourier-based analyses (Wei and Fwa, 2004; Wei et al., 2005; Chatterjee et al, 2006; Papagiannakis et al, 2007a; Papagiannakis et al, 2007b). The main challenge in wavelet analysis is the selection of the “best” mother wavelet to be used. Moreover, the instantaneous sub-band frequencies obtained from wavelet analysis are computed using low-pass and high-pass filter banks.

Pavement roughness and dynamic axle load data collected at highway speeds represent nonlinear and non-stationary data. The Fourier and wavelet transformations may not be fully sufficient to characterize roughness features and investigate the effects on vehicle dynamics. The Hilbert-Huang Transform (HHT) is a relatively new method suitable for analyzing nonlinear and non-stationary data (Huang et al., 1998). The HHT method consists of a time adaptive decomposition operation using Empirical Mode Decomposition (EMD) to break down the input signal into a finite number of Intrinsic Mode Functions (IMFs). Subsequently, a Hilbert transform is applied to each IMF to obtain the Hilbert spectrum energy. HHT analysis preserves the spatial reference of the decomposed pavement roughness and truck dynamic axle load data. Recently, the HHT method was used to characterize pavement roughness (Gagarin et al., 2004 and Wu et al., 2004), to analyze truck dynamic axle load (Zelelew and Papagiannakis, 2009), and to detect structural damages (Yang et al., 2004).

OBJECTIVE

The objective of this paper is to analyze pavement vehicle interaction using HHT. It presents an overview of the approach and the method used for computing the extent of variation over distinct ranges of frequency sub-bands. It implements this approach to analyze dataset involving roughness profile data measured with an inertial profilometer and dynamic axle load measurements obtained on board an instrumented heavy truck.

EXPERIMENTAL DATA

The experimental data utilized in the following analysis was developed by the National Research Council of Canada (Woodrooffe et al., 1986). Roughness profile data was obtained on five pavement sites with roughness IRI ranging from 0.88 to 3.17 m/km using an inertial profilometer at distance increments of 15.24 cm. The length of these sections ranged between 545 m and 900 m. A 5-axle semi-trailer equipped with an air suspension on the drive axles and a rubber suspension on the trailer axles was used to measure the dynamic axle loads. Three truck operating speeds (38, 60.5 and 79 km/h) were used. A summary of the statistics of this dataset are shown in Table 1. This dataset was previously analyzed using Fourier and wavelet transforms (Papagiannakis and Gujarathi, 1995; Papagiannakis et al, 2007a; Papagiannakis et al, 2007b).

Table 1. Experimental Data Summary Statistics (After Papagiannakis et al., 1988).

Test Site	**Roughness IRI (m/km)**	**Ride Number**[+]	**Actual Speed (km/h)**	**Dynamic Axle Load Standard Deviation (kN)***	
				Air Suspension	**Rubber Suspension**
1	0.88	3.83	38	16.51	16.52
			60.5	14.20	22.34
			79	15.14	29.35
2	1.37	3.38	38	19.31	22.73
			60.5	17.71	38.56
			79	22.52	57.89
3	1.52	3.15	38	21.27	22.32
			60.5	23.11	29.78
			79	27.96	61.88
4	1.82	2.40	38	25.77	30.33
			60.5	39.01	34.55
			79	39.80	68.99
5	3.17	2.58	38	32.01	45.52
			60.5	45.22	55.61
			79	43.12	87.45

* Mean tandem axle loads of 205.52 and 204.54 kN for the air and rubber suspensions, respectively.

[+] Ranges from 0 (impassable) to 5 (perfectly smooth).

HHT METHOD

The HHT method involves two steps. In the first step, the signal is decomposed into a finite number of Intrinsic Mode Functions (IMFs) using the method of empirical mode decomposition (EMD). In the second step, the instantaneous frequency and the amplitude of each of these IMFs are computed. The resulting time-frequency-energy representation of the signal is defined as the Hilbert spectrum (Huang et al., 1998). This decomposition allows computing the amount of variation or energy contributed by each of the wavebands.

Step One

First, the decomposition algorithm detects local maxima and minima of the input signal $s(t)$ and connects them using a cubic spline to obtain the upper envelope $u_s(t)$ and the lower envelope $l_s(t)$ of the signal, respectively. Their mean value $m_1(t)$ is given by (Huang et al., 1998):

$$m_1(t) = \frac{u_s(t) + l_s(t)}{2} \tag{1}$$

The difference between the original signal $s(t)$ and $m_1(t)$ yields the first component of the transformation $h_1(t)$:

$$h_1(t) = s(t) - m_1(t) \tag{2}$$

Additional transformation components are obtained by repeating this process, while considering the signal from the previous transformation as the original signal. Hence, the transformation after *k* steps $h_{1k}(t)$ is expressed as:

$$h_{1k}(t) = h_1(k-1) - m_{1k}(t) \tag{3}$$

After these *k* steps, the resulting $h_{1k}(t)$ is considered as the first IMF $c_1(t)$:

$$c_1(t) = h_{1k}(t) \tag{4}$$

This $c_1(t)$ has to satisfy the following IMF properties (Huang et al., 1998):

- For the entire dataset, the number of extreme and zero-crossings must either be equal or differ at most by one.
- At any point, the mean value of the envelope defined by the local maxima and the envelope defined by the local minima must be zero.

Subsequently, $c_1(t)$ is subtracted from the original signal to yield the first residual $r_1(t)$:

$$r_1(t) = s(t) - c_1(t) \tag{5}$$

This residual is treated through the same transformation process described above for the original signal to produce the second IMF transformation. Subsequent IMFs $c_j(t)$ are computed until the final residue $r_n(t)$ reduces to a monotonic or constant function.

Overall, the decomposition of the original signal $s(t)$ into n IMFs $c_j(t)$ and a residual $r_n(t)$ can be expressed as:

$$s(t) = \sum_{j=1}^{n} c_j(t) + r_n(t) \tag{6}$$

where, n is the number of IMFs.

Step Two

The second step is to apply the Hilbert transform to the decomposed IMFs. Each IMF component has a Hilbert transform expressed as:

$$y_j(t) = \frac{1}{\pi} \int_{-\infty}^{+\infty} \frac{c_j(\tau)}{t-\tau} d\tau \tag{7}$$

The analytical signal $z_i(t)$ is defined as:

$$z_j(t) = c_j(t) + \mathrm{Im}[y_j(t)] = a_j(t) e^{\mathrm{i}\theta(t)} \tag{8}$$

where, $a_j(t) = \sqrt{c_j^2(t) + y_j^2(t)}$ is the magnitude of the instantaneous amplitude and $\theta_j(t) = \arctan[y_j(t)/c_j(t)]$ is the phase of the analytic signal.

The instantaneous frequency can be related to the phase angle using:

$$\omega_j(t) = \frac{d\theta_j(t)}{dt} \tag{9}$$

Thus, the original signal can be represented as the sum of the real part of the analytical signals expressed as:

$$s(t) = \mathrm{Re}\left[\sum_{j=1}^{n} a_j(t) e^{(\mathrm{i}\int \omega_j(t) dt)} \right] \tag{10}$$

Energy Calculations

Equation 10 represents the energy and the instantaneous frequency as a function of time. This representation is called the Hilbert-Huang spectrum $H(\omega_j(t), t)$. The Hilbert spectrum energy at j^{th} level of decomposition denoted by h_j can be represented by the square of the amplitudes as:

$$h_j = \sum_{i=1}^{n} | H(\omega(t), t) |^2 \tag{11}$$

The total energy for all decompositions h_T can be computed as:

$$h_T = \sum_{j=1}^{n} h_j \tag{12}$$

Therefore, the Hilbert relative and normalized energy can be obtained using the following equations:

$$RE_j = \frac{h_j}{h_T} \times 100\% \tag{13}$$

$$NE = \frac{\sum_{j=1}^{n} h_j}{N\, dx} \tag{14}$$

where, N is the number of observations and dx is the sampling distance increment.

ANALYSIS

The HHT analysis was carried out using the signal processing toolbox in MATLAB™ (Misiti et al., 2009). Depending on the test sections, the size of the dataset ranged from 2483 to 7199 observations. This allows a maximum of 10 decomposition levels for each test site with a maximum detectable frequency of 4 cy/m (Tables 2 and 3). The level of decomposition is denoted as $h_1, h_2, h_3, \ldots h_{10}$. The actual frequency range for each sub-band was computed from the level of decomposition and the number of data points analyzed (Papagiannakis et al, 2007a; Papagiannakis et al, 2007b). Each of the decomposition levels represents the amplitude of the signal in a distinct range of frequencies. Consequently, the highest and lowest frequency sub-bands correspond to decomposition level 1 and level 10, respectively.

Table 2. Roughness Profile Sub-band Frequency.

Sub-band Levels	**Site 1**	**Site 2**	**Site 3**	**Site 4**	**Site 5**
	Frequency (cy/m)	**Frequency (cy/m)**	**Frequency (cy/m)**	**Frequency (cy/m)**	**Frequency (cy/m)**
Level 1 (h_1)	2.4354	2.4767	3.7587	2.8567	2.5605
Level 2 (h_2)	1.2177	1.2383	1.8793	1.4284	1.2802
Level 3 (h_3)	0.6088	0.6192	0.9397	0.7142	0.6401
Level 4 (h_4)	0.3044	0.3096	0.4698	0.3571	0.3201
Level 5 (h_5)	0.1522	0.1548	0.2349	0.1785	0.1600
Level 6 (h_6)	0.0761	0.0774	0.1175	0.0893	0.0800
Level 7 (h_7)	0.0381	0.0387	0.0587	0.0446	0.0400
Level 8 (h_8)	0.0190	0.0193	0.0294	0.0223	0.0200
Level 9 (h_9)	0.0095	0.0097	0.0147	0.0112	0.0100
Level 10 (h_{10})	0.0048	0.0048	0.0073	0.0056	0.0050

Table 3. Dynamic Load Sub-band Frequency; Site 5.

Sub-band Levels	**Frequency (cy/m) ***		
	Vehicle Speed		
	38 km/h	**60.5 km/h**	**79 km/h**
Level 1 (h_1)	3.0253	2.2757	2.5605
Level 2 (h_2)	1.5127	1.1378	1.2802
Level 3 (h_3)	0.7563	0.5689	0.6401
Level 4 (h_4)	0.3782	0.2845	0.3201
Level 5 (h_5)	0.1891	0.1422	0.1600
Level 6 (h_6)	0.0945	0.0711	0.0800
Level 7 (h_7)	0.0473	0.0356	0.0400
Level 8 (h_8)	0.0236	0.0178	0.0200
Level 9 (h_9)	0.0118	0.0089	0.0100
Level 10 (h_{10})	0.0059	0.0044	0.0050
***** For both air and rubber suspensions.			

The extent of roughness and dynamic axle load variation in each of the sub-band levels was summarized through an energy metric defined as the sum of squares of the observations. Therefore, the total Hilbert energy contents were computed as the sum of the squares of the decomposed coefficients in each sub-band. Further, the summation of total energy of the sub-band levels was normalized by the length of the test sections to represent normalized energy of the test site.

The overall pavement vehicle interactions can be summarized using the Hilbert normalized energy. The effects of pavement roughness and suspension types on vehicle dynamics using the truck speeds tested are illustrated in Figures 1 through 3. In general, the rubber suspension retains higher normalized energy than the air suspension regardless of vehicle speeds and pavement roughness levels. It is observed that for the rougher test sites the rubber suspension exhibits lower dynamic activity at 60.5 km/h than at 38 km/h, which is likely due to its natural frequencies in dynamic axle loads. For a given suspension type, there is a clear increase in normalize energy trend for increase in pavement roughness levels. In general, the rubber suspension impacts much higher energy per unit length traveled than the air suspension.

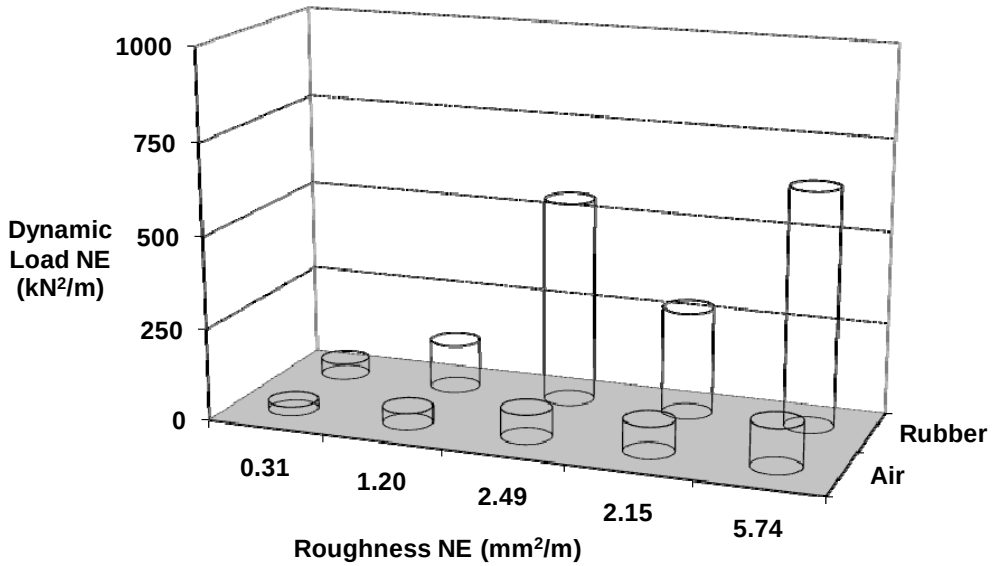

Figure 1. Effects of Pavement Roughness and Suspension Types on Truck Dynamics; Speed 38 km/h.

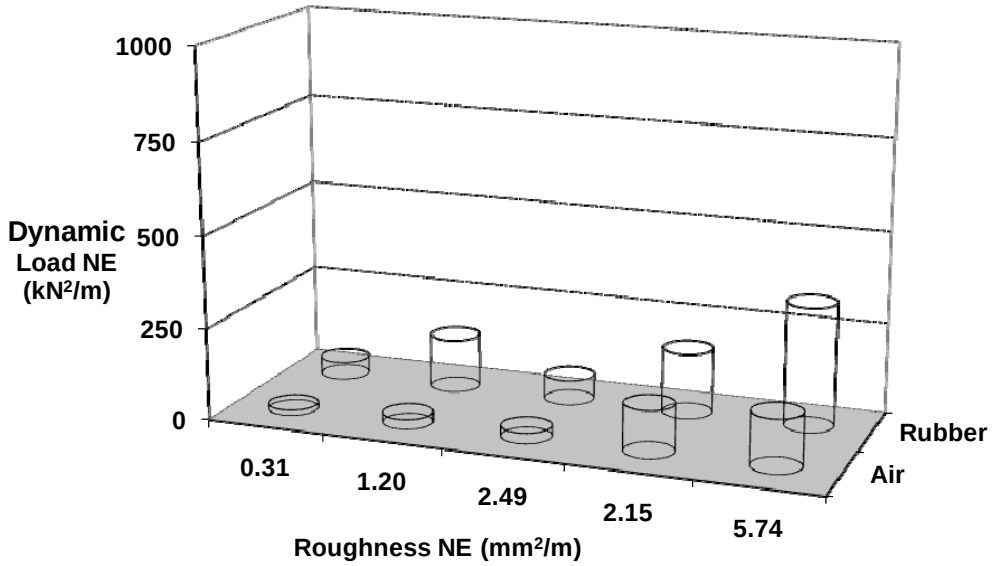

Figure 2. Effects of Pavement Roughness and Suspension Types on Truck Dynamics; Speed 60.5 km/h.

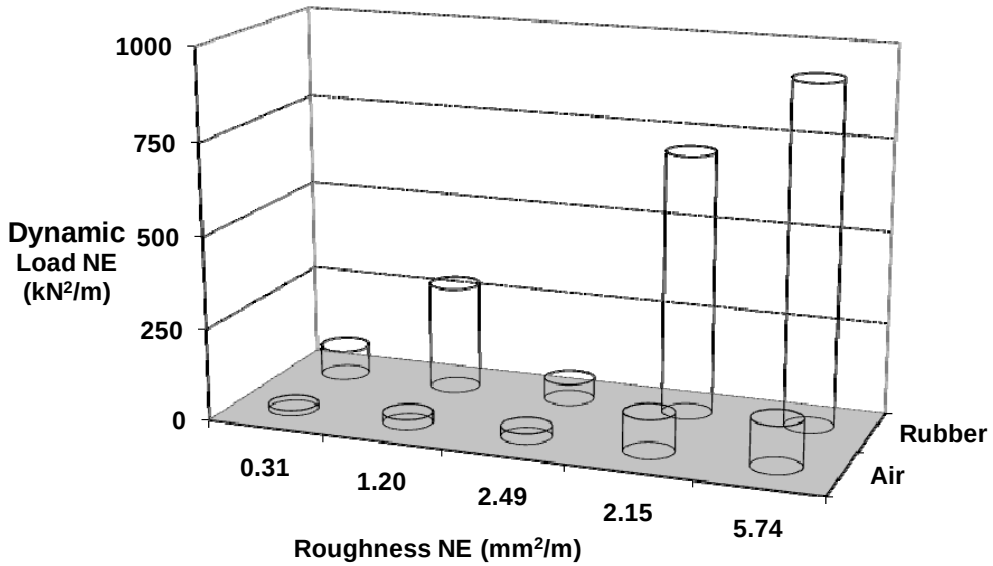

Figure 3. Effects of Pavement Roughness and Suspension Types on Truck Dynamics; Speed 79 km/h.

SUMMARY AND CONCLUSION

This paper presented an analysis of pavement vehicle interaction data using the HHT method. The data analyzed included pavement roughness profile and dynamic axle load data collected on five pavement test sites using inertial profilometer and 5-axle semi-trailer, respectively. The truck was equipped with an air suspension on the drive axles and a rubber suspension on the trailer axles. The size of the dataset analyzed allowed 10 decomposition levels with a maximum detectable frequency of 4 cy/m. The signal decomposition with this approach preserved the spatial reference of the roughness and load data and was independent of signal processing assumptions. This was a distinct advantage over the conventional Fourier and wavelet approaches. The extent of variation in roughness and dynamic axle load for each of the frequency sub-bands was summarized through Hilbert energy defined as the sum of squares of the observations (units in mm^2 and kN^2, respectively). The Hilbert normalized energy was also used to characterize the overall effects of roughness profile, suspension type, and vehicle speed on vehicle dynamics. Regardless of vehicle speeds and pavement roughness level, the rubber suspension impacted much higher energy per unit length traveled than the air suspension. In general, it was found that the HHT method is a suitable tool compared to Fourier and wavelet transforms for analysis of pavement-vehicle interaction. In conclusion, analyzing pavement roughness profile and dynamic axle loads using the HHT method provided an innovative approach to characterize pavement-vehicle interaction.

REFERENCES

1. Chatterjee, P., OBrien, E., Li, Y., and Gonzalez, A. (2006) “Wavelet domain analysis for identification of vehicle axles from bridge measurements” Computers & Structures, 84, pp. 1792-1801.
2. Gagarin N., Huang N., Oskard S., Sixbey G., and Mekemson R. (2004) “The application of Hilbert-Huang transform to the analysis of inertial profiles of pavements” International Journal of Vehicle Design, Vol. 36 (2/3), pp. 287-301.
3. Huang, N.E., Shen, Z., Long, S.R. (1998) “The empirical mode decomposition and the Hilbert spectrum for nonlinear and non-stationary time series analysis, Proc. Roy. Soc. Lond. A 454, 903–995.
4. Misiti M., Misiti, Y., Oppenheim G., and Poggi, J. M., (2009) “MATLAB Program” The Math Works Inc., Natick, Massachusetts.
5. Papagiannakis, A.T., Haas R.C.G., Woodrooffe J.H.F. and LeBlanc P. (1988) “Effects of Dynamic Load on Flexible Pavements” Transportation Research Record No. 1207, pp. 187-196.
6. Papagiannakis T., Zelelew H., and Muhunthan B. (2007a) “A Wavelet Interpretation of Pavement-Vehicle Interaction” International Journal of Pavement Engineering, 8(3), pp. 245-252.
7. Papagiannakis T., Zelelew H., and Muhunthan B. (2007b) “Wavelet Analysis of Energy Content in Pavement Roughness and Truck Dynamic Axle Loads” Transportation Research Record 1367, Transportation Research Board, National Research Council, Washington, D.C., pp. 153-159.
8. Papagiannakis T. and Gujarathi S. (1995) “A Roughness Model Describing Heavy Vehicle-Pavement Interaction” Transportation Research Record No. 1501, pp. 50-59, 1995.
9. Wei, L. and Fwa, T. F. (2004) “Characterizing Road Roughness by Wavelet Transform, Transport Research Board Record 1869, pp. 152-158.
10. Wei L., Fwa T. F. and Zhe Z. (2005) ”Wavelet Analysis and Interpretation of Road Roughness” ASCE Transportation Journal, Vol. 131, No. 2, pp. 120-130.
11. Woodrooffe F., LeBlanc A., and LePianne P. (1986) “Effect of Suspension Variations on the Dynamic Wheel Loads of a Heavy Articulated Vehicle” Road and Transportation Association of Canada, Vehicle Weights and Dimensions Study, Technical Report Vol. 11.
12. Wu H., Yao Q., and Jin Y. (2004) “Application of the Hilbert-Huang Transform to Pick up Surface Roughness” Material Science Forum, Vol. 471-472, pp. 668-671.
13. Yang J., Lei Y., Lin S., and Huang N. (2004) “Hilbert-Huang-Based Approach for Structural Damage Detection” Journal of Engineering Mechanics, Vol. 130 (1), pp. 85-95.
14. Zelelew H., and Papagiannakis T. (2009) “Analysis of Truck Dynamic Axle Loads using Hilbert–Huang Transforms” Transportation Research Record 1005, Transportation Research Board, National Research Council, Washington, D.C. (Accepted).